SLAC-PUB-13505
January 2009 LETTERS

Limits on the Superconducting Order Parameter in $NdFeAsO_{1-x}F_y$ from Scanning SQUID Microscopy

Clifford W. HICKS, Thomas M. LIPPMAN, Martin E. HUBER[1], Zhi-An REN[2], Jie YANG[2], Zhong-Xian ZHAO[2], and Kathryn A. MOLER*

Geballe Laboratory for Advanced Materials, Stanford University, Stanford, CA 94305, U.S.A.
[1]*Departments of Physics and Electrical Engineering, University of Colorado Denver, Denver, CO 80217, U.S.A.*
[2]*National Laboratory for Superconductivity, Institute of Physics and Beijing National Laboratory for Condensed Matter Physics, Chinese Academy of Sciences, P.O. Box 603, Beijing 100190, P.R. China*

(Received August 7, 2008; accepted November 14, 2008; published December 25, 2008)

Identifying the symmetry of the superconducting order parameter in the recently-discovered ferro-oxypnictide family of superconductors, RFeAsO$_{1-x}$F$_y$, where R is a rare earth, is a high priority. Many of the proposed order parameters have internal π phase shifts, like the d-wave order found in the cuprates, which would result in direction-dependent phase shifts in tunnelling. In dense polycrystalline samples, these phase shifts in turn would result in spontaneous orbital currents and magnetization in the superconducting state. We perform scanning SQUID microscopy on a dense polycrystalline sample of NdFeAsO$_{0.94}$F$_{0.06}$ with $T_c = 48$ K and find no such spontaneous currents, ruling out many of the proposed order parameters.

KEYWORDS: ferro-oxypnictides, pnictides, scanning SQUID microscopy, order parameter, NdFeAsO
DOI: 10.1143/JPSJ.78.013708

The recently-discovered ferro-oxypnictide family of superconductors includes materials with transition temperatures above 50 K[1)] and shows evidence that competing magnetism plays a key role in the superconductivity.[2–4)] Determining the superconducting order parameter (OP) is key to understanding the interactions that induce superconductivity, but the OP of the ferro-oxypnictide family of superconductors remains uncertain. We report a phase-sensitive test of the symmetry of the OP using scanning magnetic microscopy of dense polycrystalline samples.

Grain boundaries form naturally occuring Josephson junctions that can carry supercurrents. It is now well-known that the OP of the cuprate superconductors contains π phase shifts associated with the d-wave symmetry, and that a π phase shift can result upon going around a closed path in a polycrystalline sample; whether there is a π shift depends on the relative lattice and interface orientations of the grains along the loop,[5)] for example as diagrammed in Fig. 1. π-loops result in orbital frustration and spontaneous currents, as demonstrated by observation of half-integer flux quanta in tricrystal cuprate samples.[6)] In polycrystalline cuprate samples there is a finite density of π loops, which, in well-connected samples (i.e., with the intergrain Josephson penetration depth λ_J comparable to or less than the grain size), results in complex patterns of magnetization.[7)]

Proposals for the ferro-oxypnictide OP include extended-s order, with a π phase shift between the hole and electron Fermi sheets,[8–12)] $d_{x^2-y^2}$,[9,13–15)] d_{xy},[16)] p,[15,17)] $s+d$,[18,19)] and $s+id$.[19)] Phase-sensitive tests of the OP are important: because of the multiple Fermi sheets, and because time-reversal symmetry-breaking (TRSB) OPs remain a possibility, establishing the presence or absence of nodes does not definitively settle the OP symmetry.

Which OPs would result in orbital frustration in a polycrystalline sample? Any pure d order will result in a π phase shift between a and b axis tunnelling, leading to frustration. In principle a TRSB component could reduce the degree of frustration: $d_{x^2-y^2}+id_{xy}$ order on a radially symmetric band, and in a 2-D sample (the c-axes of the grains aligned), does not give frustration. However, with the electron pockets, the ferro-oxypnictide Fermi surface is not radially symmetric, and any such reduction would be minimal. p order would result in frustration with or without a TRSB component. π-shifted s order in principle could result in a π shift between a and c axis tunnelling, if different, π-shifted, sections of the Fermi surface dominate a and c axis tunnelling. Whether this is likely requires calculation. At present we must assume that an absence of spontaneous moments does not rule out π-shifted s order.

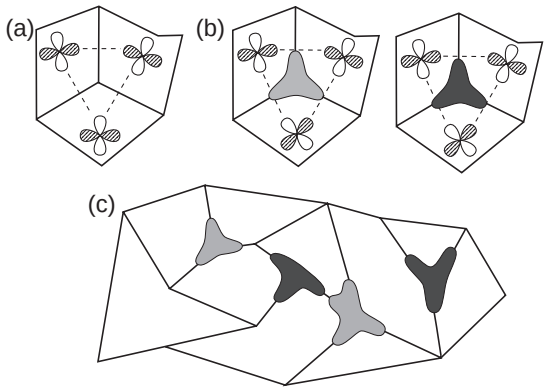

Fig. 1. Spontaneous magnetic flux generated by various configurations of grains. (a) Three coupled grains of a d-wave superconductor with no orbital frustration. The orientation of the OP in each grain is indicated; shading indicates the sign of the OP and dashed lines directions of strong intergrain tunnelling. (b) Coupled grains with orbital frustration. If λ_J is smaller than the grain size a half-flux-quantum ($\Phi_0/2$) vortex is generated, which can be positive (light) or negative (dark). (c) A polycrystalline sample with several $\Phi_0/2$ vortices, which will tend to couple antiferromagnetically.

We have performed scanning SQUID imaging of a polycrystalline sample of nominal composition NdFeAs-

Work supported in part by US Department of Energy contract DE-AC02-76SF00515
Published in the Journal of the Physical Society of Japan

$O_{0.94}F_{0.06}$ grown by a high-pressure synthesis method.[20] The superconducting transition onsets at 51 K, with a midpoint at 48 K and a 10–90% width of 2.7 K. The grains are well-coupled: magneto-optical imaging and remnant magnetization measurements on a sample from the same batch indicate a bulk critical current of $\approx$2000 A/cm^2 at 5 K.[21]

Our SQUID is a niobium-based scanning susceptometer design.[22] Figure 2(a) contains an image of the front end of the SQUID; magnetic flux is coupled into the 4.6 µm diameter pick-up coil (the inner coil), the leads to which are shielded. In this SQUID a signal of 1 $\Phi_0 = hc/2e = 2.07 \times 10^{-15}$ Wb corresponds to a mean B_z in the pick-up coil of $\approx$0.125 mT. The larger loop around the pick-up coil is a field coil; a measure of the local susceptibility can be obtained by applying a local field with this coil and measuring the response in the pick-up coil.

We polished the sample to a shiny surface using Al_2O_3 polishing paper without any lubricant. In order to allow comparison with the vacuum, we scanned an area going over the edge of the sample. Our main results, scans of the sample cooled in different fields, are shown in Fig. 2. At fields below $\approx$2 µT [panels (b)–(e)] individual vortices are clearly resolved. They appear in different places on cooling in different fields, indicating that they are not frustration-induced spontaneous moments. For confirmation that they are regular vortices, they can be integrated: after subtracting a planar background, the three vortices indicated in Fig. 2(c) integrate to, from top to bottom, 1.05, 1.00, and -1.06 Φ_0 (with a 5% systematic uncertainty due to uncertainty in the effective pick-up coil area).

The 4.4 K scans reveal other features: several surface dipoles, clusters of vortices hinting at lumps of a magnetic impurity phase, possibly beneath the surface, and a widespread mottled background. In the area indicated in Fig. 2(b), the root-mean-square amplitude of this background signal, after plane subtraction, is 1.7 mΦ_0. By lifting the SQUID slightly above the sample the sample can be heated while maintaining the SQUID below its T_c; a $T = 55$ K scan [Fig. 2(f)] confirms the presence of magnetic impurity phase. The surface dipoles also persist at 55 K while the mottled background disappears at T_c.

Figure 2(g), a scan at $\approx$100 µT, makes clear the granular nature of the sample: vortices cluster strongly in areas of weaker superconductivity.

Figure 2(h) shows sections of an isolated vortex and surface dipole from Fig. 2(c). The surface dipole provides a measure of the achieved imaging resolution: the peaks are separated by 5 µm. Assuming a 4.6-µm-diameter pick-up coil and a point-like dipole this indicates a scan height of the pick-up loop above the sample surface of $\approx$3 µm. 2-D fits to the smallest dipoles in Fig. 2(f) also indicate a scan height of $\approx$3 µm.

Figure 2(i) is a histogram of the full-width half-maxima of the vortices in Fig. 2(c). The narrowest are $\approx$8 µm. With a 4.6 µm SQUID at a scan height of 3 µm a vortex in a sample with zero penetration depth would appear with a FWHM of 6.2 µm; i.e., the 8 µm FWHMs are strongly resolution-limited. However most of the vortices have observed FWHMs in the range 10–16 µm, and most have visibly irregular shapes, suggesting that the actual vortices in the sample are spread out, with widths in the range of micrometers.

A susceptibility scan (Fig. 3) shows which areas are superconducting: over these areas the field coil is partially shielded by the Meissner screening of the sample, reducing the field coil–pick-up coil coupling (measured in Φ_0 of flux through the pick-up coil per mA of current in the field coil). These areas appear dark in the figure. The granular nature of the sample and areas of non-superconducting phase are evident. (The lower right area appears most strongly superconducting, however this is probably an artifact of topography allowing the SQUID closer to the sample.) Figure 3 also shows an electron backscatter diffraction image, a technique which reveals crystal lattice orientation, of the polished surface of a different piece of the same sample. The average grain diameter, in a circle approximation, is 5.1 µm.

At first glance the mottled background observed in Figs. 2(b)–2(e) may resemble the complex magnetization expected for orbital frustration in a polycrystalline sample. However, to the extent visible between vortices, this background is identical in Figs. 2(b)–2(e), whereas frustration-related moments are polarizeable by cooling in µT-scale applied fields.[5] Instead, the background is consistent with an uncancelled in-plane field: as indicated in Fig. 2 we must apply ≈ -3.3 µT to cancel the z-axis component of the ambient field, and a comparable in-plane component can be expected. This would result in in-plane vortices which would leak out near the surface of the inhomogeneous sample. Also, field lines above the sample would be deflected upward and downward by the surface inhomogeneity. Both effects would contribute to a mottled background signal.

Polarizable moments would lead to the Wohlleben effect, a bulk paramagnetism against the field in which the sample was cooled for fields $\lesssim 100$ µT, and which has been observed for polycrystalline cuprates.[5] To test for the Wohlleben effect in $NdFeAsO_{0.94}F_{0.06}$, we compare the average signal over the sample with the signal beyond the sample edge (in all cases the sample was cooled and scanned in the same field). The result, shown in Fig. 4, indicates diamagnetism against sub-100 µT cooling fields, consistent with an absence of polarizable moments.

Qualitative examination of the scans and the absence of the Wohlleben effect indicate an absence of orbital frustration in $NdFeAsO_{0.94}F_{0.06}$.

In the remainder of the paper, we use established modelling techniques to show quantitatively that the signal that would emerge from orbital frustration would be larger than the small mottled background field evident in Fig. 2. The observed vortex widths suggest a Josephson penetration depth λ_J comparable to the grain size, so spontaneous moments would not be well-isolated. Tightly-spaced moments would also tend to align antiferromagnetically, further reducing the expected signal at the SQUID. We estimate the expected signal from orbital frustration by modelling the grain interfaces as a long 1-D Josephson junction, with a single λ_J, divided into 0- and π-junction domains. A 1-D junction is a reasonable approximation because the grain size is comparable to the system resolution. In the narrow junction limit the phase change across the junction, $\phi(x)$, satisfies a sine-Gordon equation,

$$\frac{\partial^2 \phi}{\partial x^2} = \frac{1}{\lambda_J^2} \sin[\phi(x) + \theta(x)], \tag{1}$$

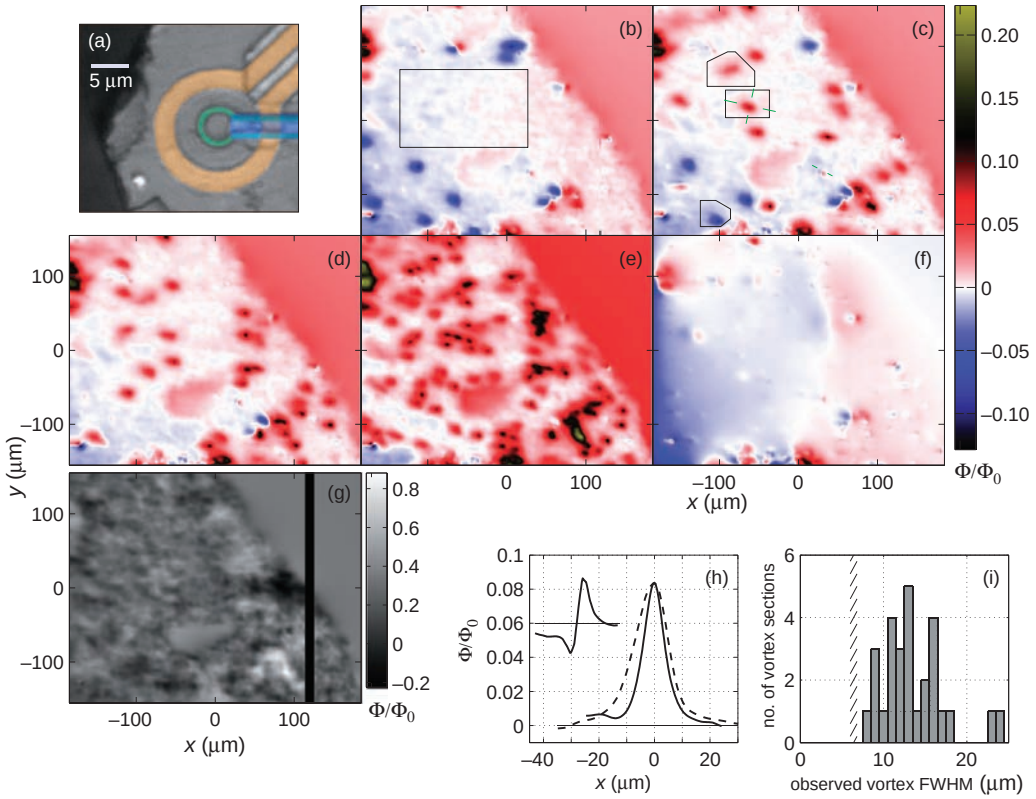

Fig. 2. (a) Optical image of the front end of the SQUID; the field coil is highlighted in orange, the pick-up coil in green, and the shield of the pick-up coil leads in blue. (b–g) Images of the magnetic flux coupled into the pick-up coil at sample temperature and applied field (b) 4.4 K, −3.3 μT; (c) 4.4, −2.7; (d) 4.4, −2.2; (e) 4.4, 0; (f) 55, 0; and (g) 4.4 K, +98 μT. An ambient z-axis field of ≈3.3 μT adds to these fields. The area indicated in (b) is used to analyze the background and the areas in (c) are integration areas (see text). (h) Cross sections along the green lines in (c): one section of a surface dipole and two of a vortex. (i) Histogram of observed FWHMs of the isolated vortices in (c); two FWHMs per vortex, along the narrow and long axes. Hatched area indicates the approximate resolution limit.

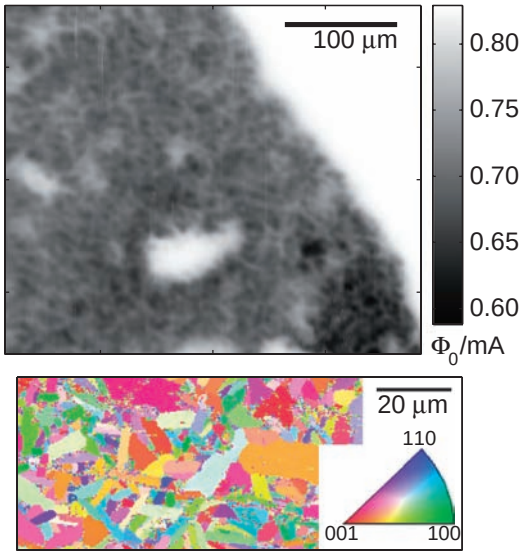

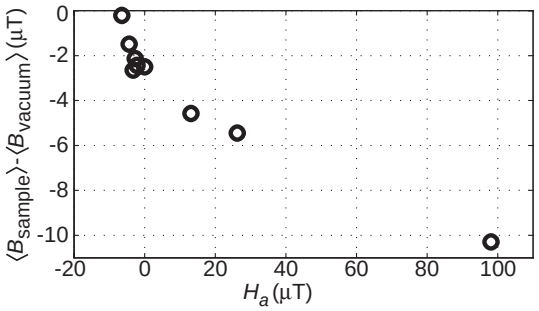

Fig. 4. From each scan, the difference between the mean B_z over the sample and in the corner farthest from the sample, against applied field (during cooling and scanning) H_a.

where $\theta(x)$ is the position-dependent frustration phase (set here to 0 or π).

Two empirical estimates of the typical λ_J for this sample are available.

$$\lambda_J = \left(\frac{\hbar c^2}{8\pi e d j_c}\right)^2, \tag{2}$$

where d is the magnetic width of the junction and j_c its critical current density. (The narrow junction limit is $d \ll \lambda_J$.) $d = d_0 + \lambda_1 + \lambda_2$, where d_0 is the actual intergrain spacing and λ_1 and λ_2 are the penetration depths of the two grains. The grain orientations being random these will fall between λ_{ab} and λ_c. λ_{ab} has been measured at ≈200 nm in $T_c \approx 50$ K Sm- and Nd-based samples,[23–25] and $\lambda_c/\lambda_{ab} \sim 5$ has been measured in $NdFeAsO_{0.90}F_{0.10}$.[26] For $j_c \sim 2000$ A/cm^2 and $d \sim 2$ μm, $\lambda_J \sim 4$ μm is obtained.

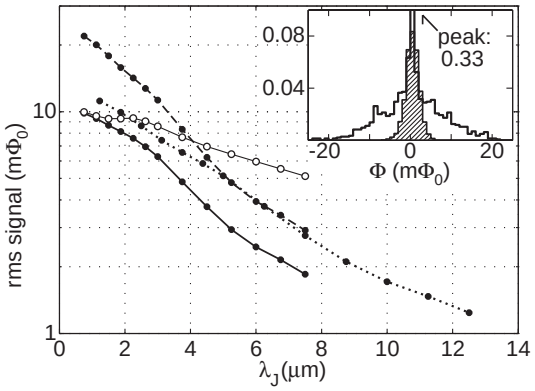

The other estimate of λ_J comes from the observed vortex widths. The soliton solution, for a vortex within the junction, to the sine-Gordon equation is obtained by setting $\theta(x)$ to zero everywhere. To extend this solution to above the sample we model it as a line of monopole sources an effective height h beneath the pick-up coil, where h is the actual scan height plus λ, and then integrate B_z over the pick-up coil area. h can be estimated from the susceptibility scan shown in Fig. 3: over the sample the field coil–pick-up coil coupling is reduced by $\approx 0.16\,\Phi_0/\mathrm{mA}$ relative to in vacuum, which would happen with the field and pick-up coils $\approx 5\,\mu\mathrm{m}$ above a hypothetical $\lambda = 0$ plane. Setting $h = 5\,\mu\mathrm{m}$, observed vortex FWHMs of 10–16 μm indicate λ_J in the range of 1–4 μm.

We simulate orbital frustration with a discretized junction 20,000 elements in length, divided into domains of mean length $L = 40$. In each domain $\theta(x)$ is set to π with probability P, and zero otherwise. $\phi(x)$ is obtained numerically as described in ref. 27. To simulate gradual cooling, the system was first solved with $\lambda_J = 200$, then λ_J was reduced in steps to 10, taking the solution from the previous step (with a small perturbation to disrupt unstable solutions) as the starting point for the next. L and λ_J are then scaled to lengths in micrometers, and the solutions are again extended to above the sample by modelling as a line of monopole sources.

The results of this simulation are shown in Fig. 5, and although it is an approximate model the simulation shows that for a wide range of reasonable choices of L, h, and λ_J a signal comparable to or larger than the observed background would result: the fixed background is very unlikely to be obscuring an orbital frustration signal. The inset compares the expected signal distribution for the particular case $P = 0.25$ and L, h, $\lambda_J = 3$, 6, 3 μm, respectively, with the observed background (after plane subtraction) in the area indicated in Fig. 2(b).

We have demonstrated that there very likely are no π phase shifts between tunnelling in different directions in $NdFeAsO_{0.94}F_{0.06}$, making p and d orders unlikely. s order, π-shifted or not, and $s + d$ order where the d component is small are not ruled out by our result.

Acknowledgments

This project was supported by the U.S. Department of Energy (DE-AC02-76SF00515). We thank David Larbalestier, Alex Gurevich, and Doug Scalapino for useful discussion. We also thank Fumitake Kametani and David Larbalestier for providing the EBSD image.

1) Several $T_c > 50$ K materials are now known, for example in Z. A. Ren, W. Lu, J. Yang, W. Yi, X. L. Shen, C. Zheng, G. C. Che, X. L. Dong, L. L. Sun, F. Zhou, and Z. X. Zhao: Chin. Phys. Lett. **25** (2008) 2215.
2) G. F. Chen, Z. Li, D. Wu, G. Li, W. Z. Hu, J. Dong, P. Zheng, J. L. Luo, and N. L. Wang: Phys. Rev. Lett. **100** (2008) 247002.
3) C. de la Cruz, G. Huang, J. W. Lynn, J. Li, W. Ratcliff II, J. L. Zaretsky, H. A. Mook, G. F. Chen, J. L. Luo, N. L. Wang, and P. Dai: Nature **453** (2008) 899.
4) R. H. Liu, G. Wu, T. Wu, D. F. Fang, H. Chen, S. Y. Li, K. Liu, Y. L. Xie, X. F. Wang, R. L. Yang, L. Ding, C. He, D. L. Feng, and X. H. Chen: Phys. Rev. Lett. **101** (2008) 087001.
5) M. Sigrist and T. M. Rice: Rev. Mod. Phys. **67** (1995) 503.
6) C. C. Tsuei, J. R. Kirtley, C. C. Chi, L. S. Yu-Jahnes, A. Gupta, T. Shaw, J. Z. Sun, and M. B. Ketchen: Phys. Rev. Lett. **73** (1994) 593.
7) J. R. Kirtley, A. C. Mota, M. Sigrist, and T. M. Rice: J. Phys.: Condens. Matter **10** (1998) L97.
8) I. I. Mazin, D. J. Singh, M. D. Johannes, and M. H. Du: Phys. Rev. Lett. **101** (2008) 057003.
9) K. Kuroki, S. Onari, R. Arita, H. Usui, Y. Tanaka, H. Kontani, and H. Aoki: Phys. Rev. Lett. **101** (2008) 087004.
10) F. Wang, H. Zhai, Y. Ran, A. Vishwanath, and D. H. Lee: arXiv:0807.0498.
11) W. Q. Chen, K. Y. Yang, Y. Zhou, and F. C. Zhang: arXiv:0808.3234.
12) A. V. Chubukov, D. V. Efremov, and I. Eremin: Phys. Rev. B **78** (2008) 134512.
13) Z. J. Yao, J. X. Li, and Z. D. Wang: arXiv:0804.4166.
14) Z. Y. Weng: arXiv:0804.3228.
15) X. L. Qi, S. Raghu, C. X. Liu, D. J. Scalapino, and S. C. Zhang: arXiv:0804.4332.
16) Q. M. Si and E. Abrahams: Phys. Rev. Lett. **101** (2008) 076401.
17) P. A. Lee and X. G. Wen: arXiv:0804.1739.
18) K. Seo, B. A. Bernevig, and J. Hu: Phys. Rev. Lett. **101** (2008) 206404.
19) W. C. Lee, S. C. Zhang, and C. J. Wu: arXiv:0810.0887.
20) Z. A. Ren, J. Yang, W. Lu, W. Yi, X. L. Shen, Z. C. Li, G. C. Che, X. L. Dong, L. L. Sun, F. Zhou, and Z. X. Zhao: Europhys. Lett. **82** (2008) 57002.
21) A. Yamamoto, A. A. Polyanskii, J. Jiang, F. Kametani, C. Tarantini, F. Hunte, J. Jaroszynski, E. E. Hellstrom, P. J. Lee, A. Gurevich, D. C. Larbalestier, Z. A. Ren, J. Yang, X. L. Dong, W. Lu, and Z. X. Zhao: Supercond. Sci. Technol. **21** (2008) 095008.
22) M. E. Huber, N. C. Koshnick, H. Bluhm, L. J. Archuleta, T. Azua, P. G. Björnsson, B. W. Gardner, S. T. Halloran, E. A. Lucero, and K. A. Moler: Rev. Sci. Instrum. **79** (2008) 053704.
23) S. Weyeneth, U. Mosele, N. D. Zhigadlo, S. Katrych, Z. Bukowski, J. Karpinski, S. Kohout, J. Roos, and H. Keller: arXiv:0806.1024.
24) R. Khasanov, H. Luetkens, A. Amato, H. H. Klauss, Z. A. Ren, J. Yang, W. Lu, and Z. X. Zhao: Phys. Rev. B **78** (2008) 092506.
25) A. J. Drew, F. L. Pratt, T. Lancaster, S. J. Blundell, P. J. Baker, R. H. Liu, G. Wu, X. H. Chen, I. Watanabe, V. K. Malik, A. Dubroka, K. W. Kim, M. Roessle, and C. Bernhard: Phys. Rev. Lett. **101** (2008) 097010.
26) C. Martin, R. T. Gordon, M. A. Tanatar, M. D. Vannette, M. E. Tillman, E. D. Mun, P. C. Canfield, V. G. Kogan, G. D. Samolyuk, J. Schmalian, and R. Prozorov: arXiv:0807.0876.
27) J. R. Kirtley, K. A. Moler, and D. J. Scalapino: Phys. Rev. B **56** (1997) 886.